Evaluating and Predicting the Land Use Land Cover Changes and its Impact on Land Surface Temperature using CA-Markov model: A study of District Mardan, Pakistan

Muhammad Awais Khan, Atta Ur Rahman, Zahid Khan, Zain Sultan, Faheema Marwat, Tabassum Naz, Bushra Zahid
Department of Geography & Geomatics (GIS/RS), University of Peshawar, Pakistan.

Citation | Khan. M. A, Rahman. A. U, Khan. Z, Sultan. Z, Marwat. F, Naz. T, Zahid. B, "Evaluating and Predicting the Land Use Land Cover Changes and its Impact on Land Surface Temperature using CA-Markov model: A study of District Mardan, Pakistan", IJIST, Special Issue pp. 352-372, June 2024
Received | June 07, 2024; **Revised |** June 11, 2024; **Accepted |** June 14, 2024; **Published |** June 23, 2024.

The Rapid population growth is a global phenomenon that reshapes landscapes and impacts environmental conditions. This study aims to analyze the effects of urbanization on Land Use Land Cover (LULC) changes and their impact on Land Surface Temperature (LST) in District Mardan from 2002 to 2022, while also predicting future LULC and LST changes for the year 2042. Utilizing remotely sensed data and Geographic Information Systems (GIS), the study evaluates the correlation between the conversion of natural landscapes to built-up areas and the resulting changes in LST. The primary objectives are to investigate LULC changes over the past two decades, examine how these changes influence LST, and forecast future LULC and LST trends using the CA-Markov model in IDRISI SILVA software for 2042. The analysis of LULC changes from 2002 to 2022 reveals a significant increase in built-up areas and a decrease in vegetation. Built-up land expanded from 10.10% in 2002 to 16.28% in 2022, representing a 6% increase, while vegetation cover decreased by nearly 10% of the total land cover. Concurrently, LST data show that areas experiencing high temperatures have increased since 2002. In 2002, 37% of the total area had temperatures below 30°C, whereas this figure dropped to 28% by 2022. Correlation between LULC and LST indicates that barren surfaces and built-up regions experience higher temperatures, while areas with vegetation and water exhibit lower and more moderate temperatures. The CA-Markov model forecasts that built-up land will increase by 19% by 2042, continuing the current trend, while vegetation areas are expected to decrease by an additional 4% from their 2022 levels. The LST analysis suggests a further increase in high-temperature areas, with a predicted 3% decrease in low-temperature regions. This research highlights the historical trajectory of urbanization and its thermal effects in District Mardan, providing critical insights for sustainable land-use planning and strategies to mitigate urban heat island effects in the coming decades.

Keywords: LULC; GIS; Land Surface Temperature; Urban Expansion; CA-Markov Chain Analysis.

Introduction:

The modification of Earth's terrestrial surface by human activities is widely referred to as Land Use Land Cover (LULC) change [1]. LULC is influenced by a combination of ecological factors, such as the geological structure, altitude, and slope, as well as socio-economic, technological, and institutional factors that significantly impact land-use patterns in a given area. LULC encompasses various ways in which land is utilized, including agriculture, conservation, development, recreation, wildlife habitats, and urbanization. It also reflects the outcomes of human-environment interactions shaped by socioeconomic dynamics and climate change processes [2]. Changes in land use and land cover play a crucial role in altering the environment on both local and global scales [3]. These changes result from human activities, rapid urban growth, and economic development [4].

Cities have existed since the early human settlements in Mesopotamia between 4000 BC and 3000 BC, and now more than half of the world's population resides in urban areas. As societies strive for sustainability, there is a shift towards urban living, with people becoming more like 'metro sapiens' [5]. Urbanization significantly affects local weather and climate. Urban climate studies have long examined the differences in ambient air temperature between cities and their surrounding rural areas, a phenomenon known as the Urban Heat Island (UHI) effect [5]. The UHI effect arises primarily from changes to the land surface, with urban temperatures typically being 2–5 degrees Celsius higher than those in rural areas [6]. The intensity of land surface temperature is closely linked to land use and land cover patterns, including building roofs, paved surfaces, vegetation, and bare ground [7]. The replacement of vegetative cover with built-up infrastructure contributes to the UHI effect, negatively impacting urban residents' daily lives and activities. Research on LST patterns and their relationship with land cover has been conducted in cities such as Guangzhou and urban clusters in the Zhejiang Delta, China, using satellite-derived radiant temperature data to study surface temperature heat islands [8].

The CA-Markov model is a spatial transformation tool that integrates the stochastic temporal Markov approach with the stochastic spatial cell automata strategy to simulate temporal and spatial land use changes [9]. This model directs temporal changes in land use classes through the Markov chain process, utilizing transition matrices [10]. Spatial changes are managed by transition potential maps, neighborhood configurations, and local transition rules during the CA modeling process [11]. The CA-Markov model benefits from the Markov chain for predicting land use change quantities and the dynamic spatial simulation provided by the CA model [12]. Additionally, the CA-Markov model addresses the limitations of inadequate socioeconomic, statistical, and historical data [14].

Objectives:

- To analyze the land use and land cover (LULC) of the study area and assess changes from 2002 to 2022.
- To investigate the spatial distribution and variations in land surface temperature (LST) across the study area and evaluate the impact of LULC changes on LST.
- To forecast future LULC changes and LST for the year 2042 using the CA-Markov model.

Novelty Statement:

The title of the current study explores a novel concept where changes in land use and land cover (LULC) are driven by human activities, particularly due to population growth in the study area from 1981 to 2023, as reported by census data. As the population increases, corresponding changes in LULC are expected, which in turn impact the land surface temperature (LST) of the area. The primary objective of this research is to investigate the dynamics of LULC and the factors influencing LST. This study aims to analyze recent LULC dynamics and predict future trends based on current data using the CA-Markov model.

Material and Methods:

Study Area:

The study area, Mardan District, is located in the Peshawar Valley and has historical significance as part of the ancient Gandhara Kingdom. Originally part of the Peshawar District until 1937, Mardan became an independent district in that year. Geographically, the district is situated between latitudes 34° 04' 40" N and 34° 31' 51" N, and longitudes 71° 49' 05" E and 72° 26' 04" E. It is bordered to the north by Buner and Malakand districts, to the east by Swabi and Buner districts, to the south by Nowshera District, and to the west by Charsadda and Malakand districts, as depicted in Figure 1. The total area of the district is 1,632 km². According to the 1998 census, the population was 1,460,100. This number increased to 2,373,399 in the 2017 census and reached 2,744,898 by the 2023 census.

Climatic conditions in the study area are based on data from the Risalpur station, which is nearby and has similar topographic features. The average temperature is 22.2°C, and the annual precipitation averages 559 mm. Stream flows generally move from north to south, with most draining into the Kabul River. Key streams include Kalpani, which originates in Baizai and flows south to join the Kabul River, and other significant streams such as Baghiari Khawar, Muqam Khawar from Sudham Valley, and Naranji Khawar from the Narangi Hills. The primary source of irrigation water is the canal system, with the upper Swat Canal serving most of the district and the lower Swat Canal irrigating the southwestern parts. Additional irrigation sources include tube wells and lift irrigation (GOP, 1998).

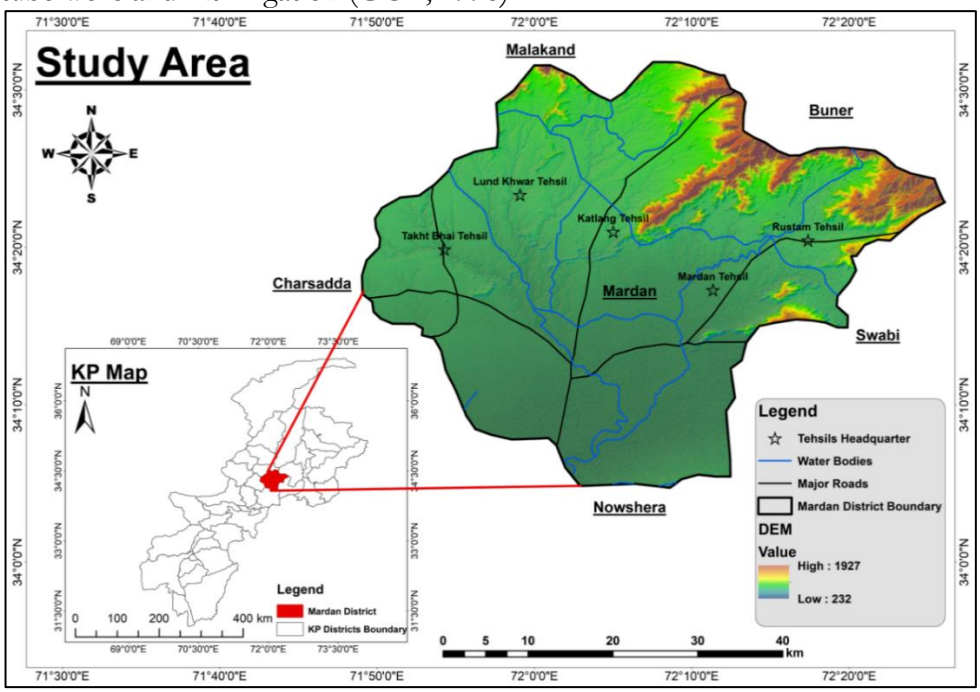

Figure 1: Location Map of the Study Area

Data Collection and Analysis:

The first step in the process is data acquisition, where satellite imagery is sourced from the USGS, specifically Landsat 7 and 8, to assess Land Use Land Cover (LULC) and Land Surface Temperature (LST). The second step involves analysis using the CA-Markov Chain model to simulate the 2042 scenario. The CA-Markov model, implemented in IDRISI Silva software, operates on a cellular automata basis. This model uses historical data trends and changes to predict future scenarios. Markov Chain analysis identifies past changes in the data, which the CA-Markov model then uses to simulate future conditions. The third step is analyzing the results of the CA-Markov simulation, focusing on LULC changes and their direct impact on LST. The fourth step involves correlating LST with various spectral and satellite indices,

including NDVI (Normalized Difference Vegetation Index), NDBI (Normalized Difference Built-up Index), NDWI (Normalized Difference Water Index), SAVI (Soil-Adjusted Vegetation Index), and BI (Brightness Index). Finally, the fifth step consists of extracting and analyzing changes from previous studies and comparing them with data from the subsequent study year.

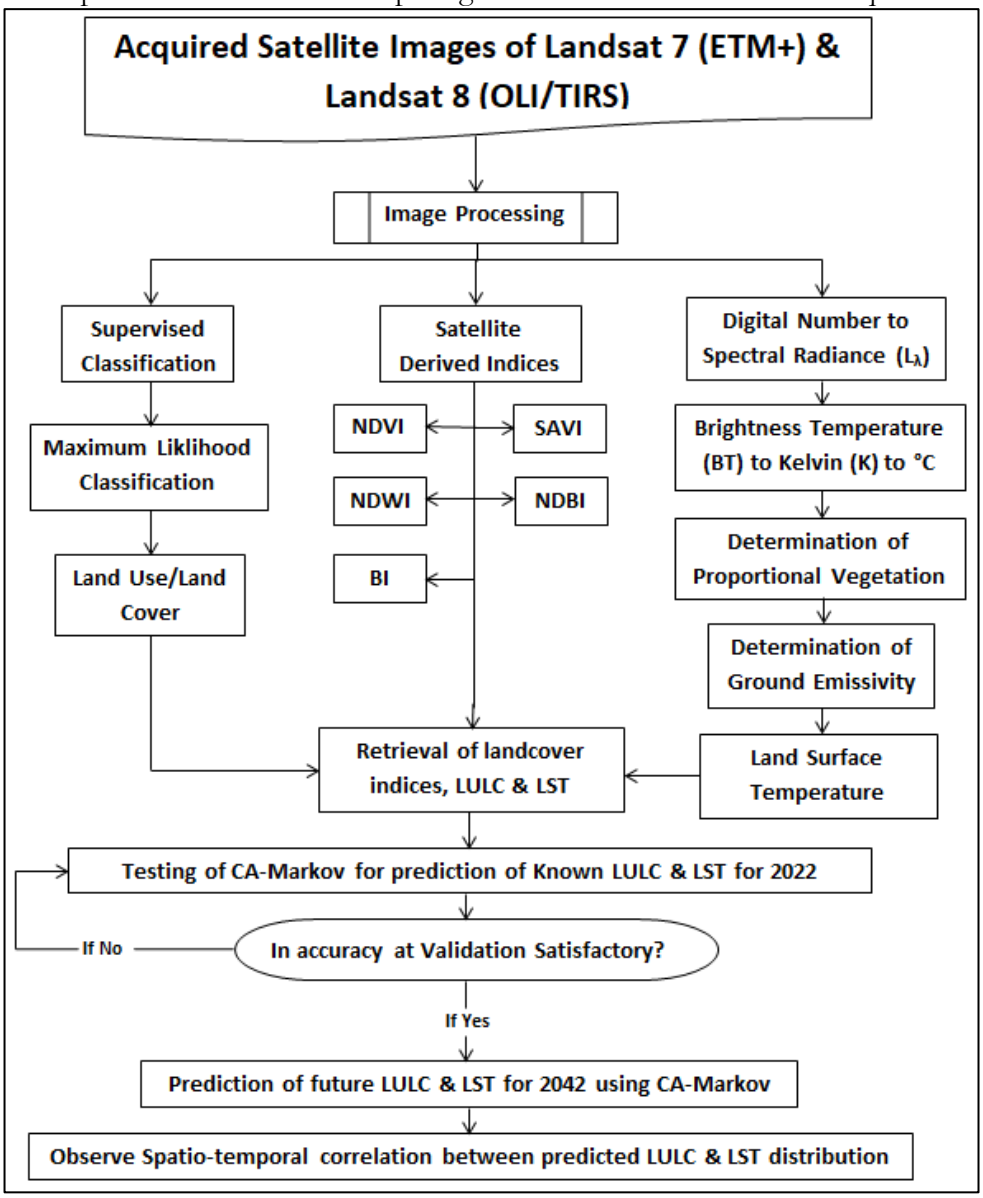

Figure 2: Flow Chart

Image Classification:

The Maximum Likelihood Classification (MLC) algorithm is a widely used method for classification in remote sensing. This algorithm requires a signature file with a `.gsg` extension as input. The MLC approach involves modifying and correlating the signature of each class to accurately classify raster images into distinct categories. By applying MLC, a classified image is generated, with the results automatically categorized as a raster layer in ArcMap.

Extraction of LST from Thermal Band:

To determine Land Surface Temperature (LST), it is necessary to convert sensor measurements into physical quantities. Sensors record the intensity of electromagnetic radiation for each pixel as digital numbers (DNs). These DNs must be converted into meaningful real-world units such as radiance (Watts), reflectance, or brightness temperature. The following

procedure was used to extract land surface temperature from the thermal bands of Landsat imagery.

Conversion of Digital Number (DN) to Spectral Radiance:

Every object with a temperature above absolute zero emits thermal electromagnetic energy. The data captured by thermal sensors can be converted to at-sensor radiance using the radiance rescaling factors provided in the metadata file.

$$L_\lambda = M_L Q_{cal} + A_L \quad (1)$$

Where \(L_\lambda \) represents the TOA spectral radiance (Watts/(m² * sr * μm)); \(ML \) is the band-specific multiplicative rescaling factor from the metadata (RADIANCE_MULT_BAND_x, where x denotes the band number).

A_L =Band-specific additive rescaling factor from the metadata (RADIANCE_ADD_BAND_x, where x is the band number);

Q = Quantized and calibrated standard product pixel values (DN)

Conversion to At-Satellite Brightness Temperature:

Band data can be converted from spectral radiance to top-of-atmosphere brightness temperature using the thermal constants provided in the metadata file, as described by Equation 2.

$$Tb = K*2 / \ln (k\ 1 / L\lambda + 1) \quad (2)$$

Where \(T \) or \(BT \) represents the top-of-atmosphere brightness temperature (K); \(L_{\lambda} \) denotes the TOA spectral radiance (Watts/(m² * sr * μm)); \(K1 \) is the band-specific thermal conversion constant from the metadata (K1_CONSTANT_BAND_x, where \(x \) is the thermal band number); and \(K2 \) is the band-specific thermal conversion constant from the metadata (K2_CONSTANT_BAND_x, where \(x \) is the thermal band number).

Land Surface Temperature:

Land surface temperature was retrieved using a single-channel algorithm, which utilizes a single thermal band from the dataset. Since the temperature obtained through this method is referenced to a blackbody, corrections for land surface emissivity are necessary. Emissivity can be derived from the Normalized Difference Vegetation Index (NDVI). The emissivity-corrected land surface temperature was calculated using the procedure outlined in Equation 3.

$$LST = Tb / [1 + \{(\lambda * Tb / \varrho) * \ln\epsilon\}] \quad (3)$$

Where Tb = At - Satellite temperature; w = wavelength of emitted radiance; p= h * c / s ($1.438 * 10^{-2}$ m K); h =Planck's constant ($6.626 * 10^{-34}$ Js); s = Boltzmann Constant; c = velocity of light ($2.998 * 10^{8}$ m/s); e = Emissivity.

Land surface emissivity (LSE) is defined as the ratio of the energy radiated from a material's surface to the energy radiated from a blackbody (a perfect emitter) at the same temperature, wavelength, and viewing conditions. It can be calculated using the following equation:

$$LSE = 0.004 * PV + 0.986 \quad (4)$$

Where PV means proportion of vegetation and can be calculated using equation 5:

$$PV = \sqrt{(NDVI - NDVI_{min} / NDVI_{max} - NDVI_{min})}$$

Here's the modified and refined paragraph:

To convert the retrieved land surface temperature (LST) from Kelvin to Celsius, subtract 273.15 from the temperature in Kelvin. This conversion is based on the relationship where 0 degrees Celsius equals 273.15 Kelvin. The conversion can be performed using Equation 5.

$$LST - 273.15 \quad (5)$$

Result and Discussion:

Spatio-Temporal LULC Trend:

Figures 3 and 4 illustrate the changes in land use and land cover (LULC) in the Mardan district from 2002 to 2022. Figure 3 shows significant changes in the built-up area in the city's

central region in 2002, indicating the early stages of urban expansion. By 2022, as depicted in Figure 4, there was a notable increase in the built-up area, primarily concentrated in the district center. This period also saw a decrease in vegetation, likely due to reduced rainfall. Additionally, smaller built-up areas began to appear throughout the region, suggesting irregular urban sprawl. The substantial growth in built-up areas can be attributed to numerous housing developments in Mardan and neighboring cities between 2002 and 2022. This rapid urbanization led to a significant reduction in plant cover, highlighting the trade-off between urban expansion and green spaces. Table 1 provides a quantitative summary of the major LULC changes between 2002 and 2022, based on the Maximum Likelihood Classification (MLC) algorithm. The data reveals a considerable increase in the built-up area, from 165.47 km² (10.10% of the total area) to 266.70 km² (16.28%). Concurrently, there were decreases in vegetative areas, with a slight increase or stability in barren terrain. Water bodies expanded from 25.03 km² (1.53%) to 49.61 km² (3.03%), while barren land increased slightly from 518.60 km² (31.67%) to 528.46 km² (32.27%). Vegetative areas decreased from 928.76 km² (56.70%) to 793.09 km² (48.42%).

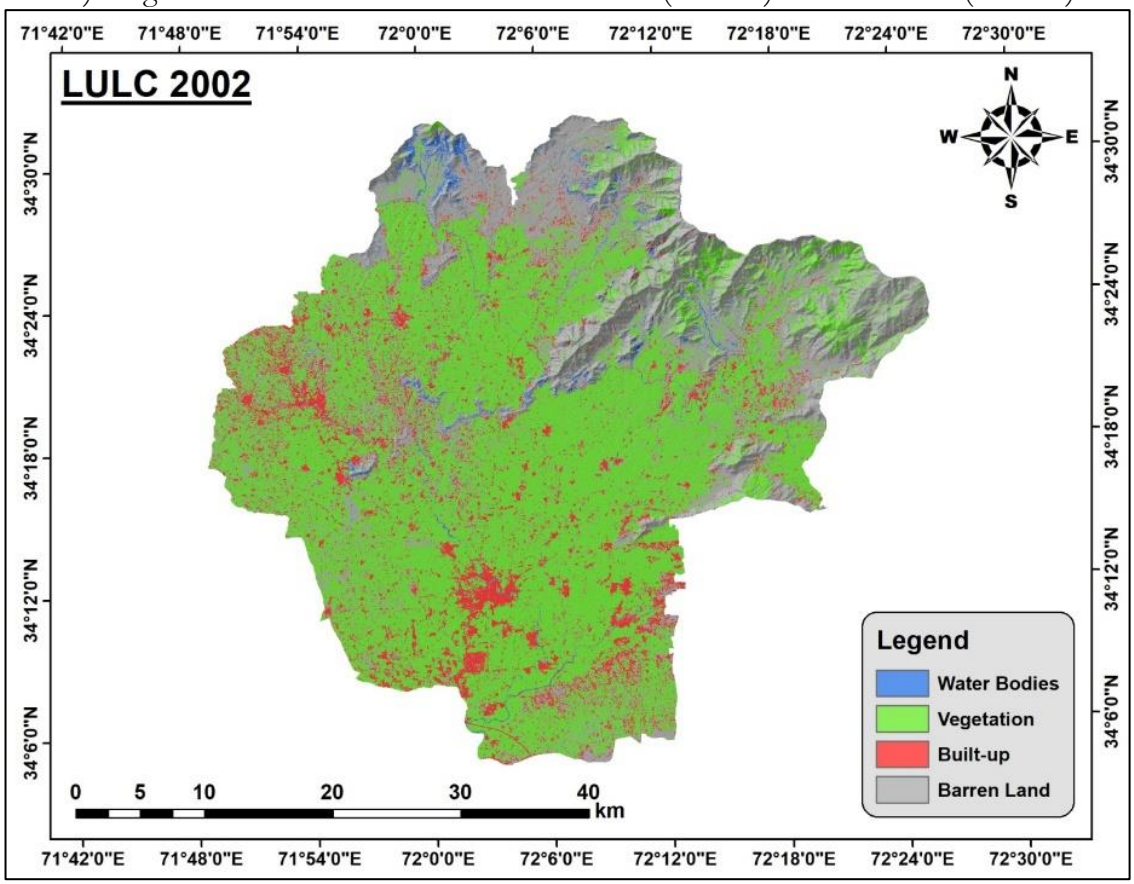

Figure 3: LULC of District Mardan 2002

Spatio-Temporal Changes in LULC from 2002 to 2022:

Over the 20-year period from 2002 to 2022, the Mardan district experienced significant changes in land use and land cover (LULC) across various categories. This research utilizes statistical data and geographical maps to illustrate the evolution of the landscape, focusing on areas where changes have occurred and excluding regions that remain unchanged.

Barren Land (BA) to Built-up Land (BU):

Between 2002 and 2022, approximately 50.70 km², or about 3.10% of the total area, of undeveloped land was converted into built-up land. This transition highlights the growth of urban areas and infrastructure improvements over the past 20 years. The expansion of residential, commercial, and industrial developments, driven by economic growth and

population increase, is the primary factor behind this increase in built-up areas. These changes are illustrated on the map as orange patches, indicating urbanization in regions previously unused or sparsely vegetated.

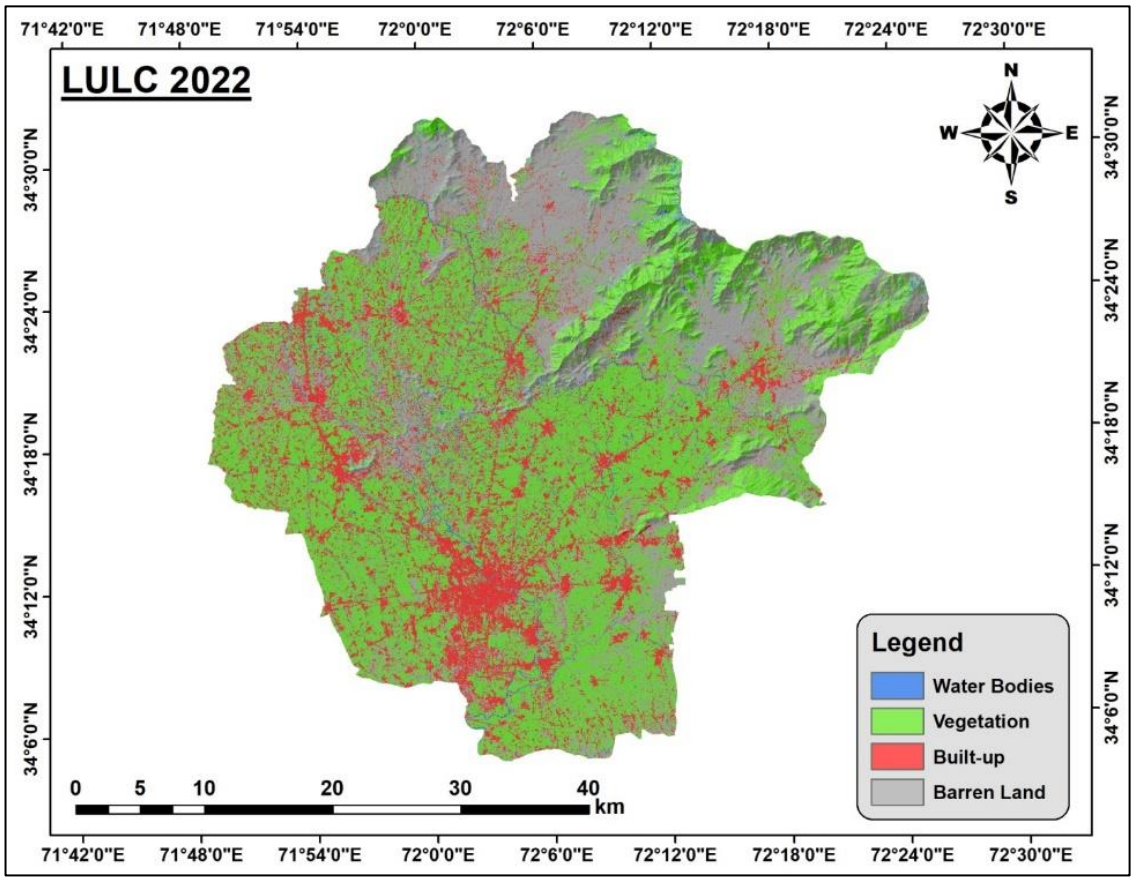

Figure 4: LULC of District Mardan 2022

Table 1: Temporal changes of LULC from 2002 to 2022

LULC	2002		2022	
Classes Names	Area in Km²	%	Area in Km²	%
Water Bodies	25.03	1.53	49.61	3.03
Vegetation	928.76	56.71	793.09	48.42
Built-up	165.47	10.10	266.70	16.28
Barren Land	518.60	31.66	528.46	32.27

Barren Land (BA) to Vegetation Land (VG):

Approximately 177.63 km², or 10.85% of the total area, has transformed from barren land to vegetated land. This significant change is likely due to reforestation efforts, agricultural expansion, or natural vegetation restoration. Increasing plant cover is essential for improving ecological balance, enhancing biodiversity, and reducing soil erosion. This shift reflects a growing recognition of the value of green spaces and their benefits.

Barren Land (BA) to Water Bodies (WB):

A less pronounced but notable change is the conversion of around 12.38 km² (0.76% of the total area) of barren land into water bodies. This transformation may result from new water management projects, such as ponds or reservoirs, designed to meet irrigation needs and improve water availability. Although less dramatic than other changes, this shift is significant for managing the district's water resources.

Vegetation Land (VG) to Barren Land (BA):

Conversely, 95.59 km², or 5.84% of the total area, has transitioned from vegetated land to barren land. This deterioration could be attributed to natural disasters, overgrazing, unsustainable agricultural practices, or deforestation. Addressing these issues requires efforts to rehabilitate degraded areas and implement sustainable land management practices.

Vegetation Land (VG) to Built-up Land (BU):

Red patches on the map represent approximately 146.16 km² (8.93% of the total area) of land that has been converted from vegetation to built-up areas. This development reflects ongoing urban sprawl, with housing and commercial spaces expanding into formerly agricultural or wooded areas. While indicative of economic growth, it underscores the importance of planning urban development to balance expansion with environmental preservation.

Water Bodies (WB) to Barren Land (BA):

A small but notable change involves the conversion of around 1.97 km² of water bodies to barren land, accounting for 0.12% of the total area. This transformation may be due to reduced water levels, sedimentation, or the drying up of water bodies, potentially influenced by climate change. Preserving existing water bodies is crucial for maintaining hydrological balance and supporting local ecosystems.

Water Bodies (WB) to Vegetation Land (VG):

Finally, the conversion of about 0.96 km² (0.06% of the total area) of water bodies into vegetation indicates areas where water bodies have either diminished or been filled in, leading to vegetative growth. While this shift may benefit native species, it highlights the need to monitor changes in water resource availability.

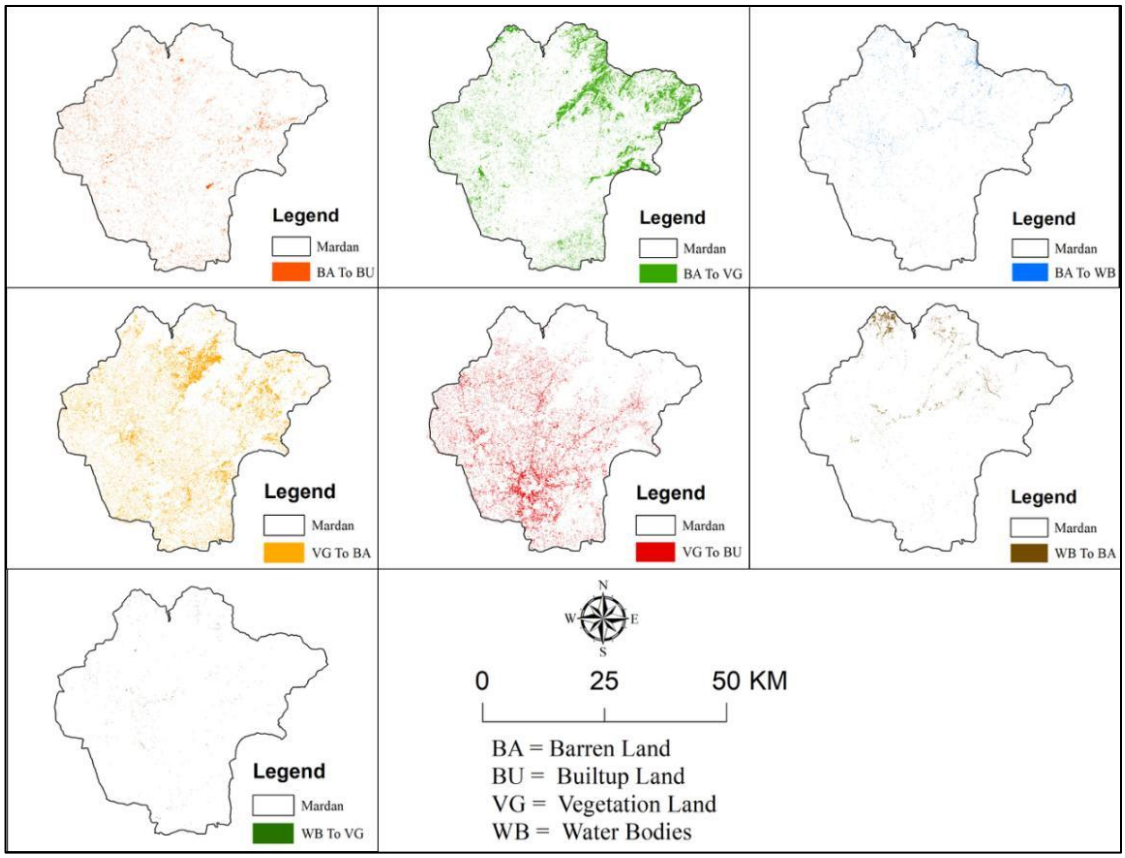

Figure 5: Maps of LULC change from 2002 to 2022

Table 2: Change in LULC statistics from 2002 to 2022

Class 2002	Class 2022	Change Classes	Change Area Sq.km	Change %
Barren Land	Barren Land	No change	273.17	16.69
Barren Land	Built-up	BA To BU	50.70	3.10
Barren Land	Vegetation	BA To VG	177.63	10.85
Barren Land	Water Bodies	BA To WB	12.38	0.76
Built-up	Built-up	No change	161.23	9.85
Vegetation	Barren Land	VG To BA	189.09	11.55
Vegetation	Built-up	VG To BU	128.82	7.87
Vegetation	Vegetation	No change	620.76	37.92
Water Bodies	Barren Land	WB To BA	15.76	0.96
Water Bodies	Vegetation	WB To VG	2.72	0.17
Water Bodies	Water Bodies	No change	4.60	0.28

Observed LST from 2002 to 2022 Using Landsat Data:

Since 2002, the Land Surface Temperature (LST) in Mardan district has shown a significant increase. Figures 6 and 7 illustrate that in 2002, the average temperature in the region was between 28 and 31°C and 31 and 33°C. By 2022, the most common temperature ranges had shifted to 31–33°C, 33–35°C, and 35–41°C. Initially, in 2002, LST values ranged from 25°C to 36°C, indicating considerable temperature variability across the area. However, by 2022, this range had expanded significantly to between 20°C and 41°C. This dramatic rise highlights the increasing temperatures, particularly in urban areas, and underscores the growing warmth of the district.

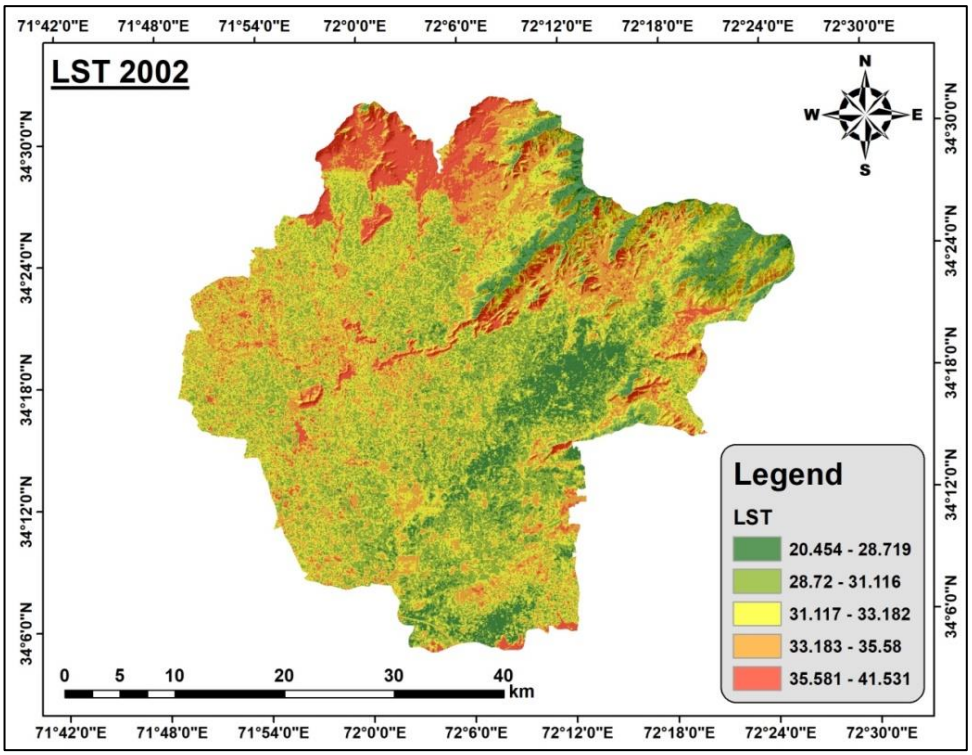

Figure 6: LST Map of 2002

The data for 2022, as shown in Figure 8, reveal a temperature increase that extends across the city's borders, elevating temperatures over a large portion of the area. Around one-third of the city experienced temperatures between 31 and 35°C and 35 and 41°C. Over time, regions with higher temperatures have expanded, while those with lower temperatures have diminished. In 2002, most of the region had temperatures between 20 and 28°C, but by 2022, Mardan City saw temperatures ranging from 35 to 41°C. This represents a temperature increase

of up to 12°C over a 20-year period. Table 3 provides an overview of LST changes between 2002 and 2022. The proportion of areas with temperatures between 20 and 23°C decreased by about 3% during this period, while there was a notable 4% increase in areas with high LSTs (35–41°C). This suggests significant surface warming in Mardan City over the past few decades.

Table 3: Temporal trend of LST observed in 2002 & 2022

LST	2002		2022	
Classes Names	**Area in km^2**	**%**	**Area in km^2**	**%**
20.454 - 28.719	147.94	9.03	100.05	6.11
28.72 - 31.116	466.99	28.51	360.95	22.05
31.117 - 33.182	511.98	31.26	493.15	30.13
33.183 - 35.58	362.40	22.13	426.59	26.06
35.581 - 41.531	148.54	9.07	256.14	15.65

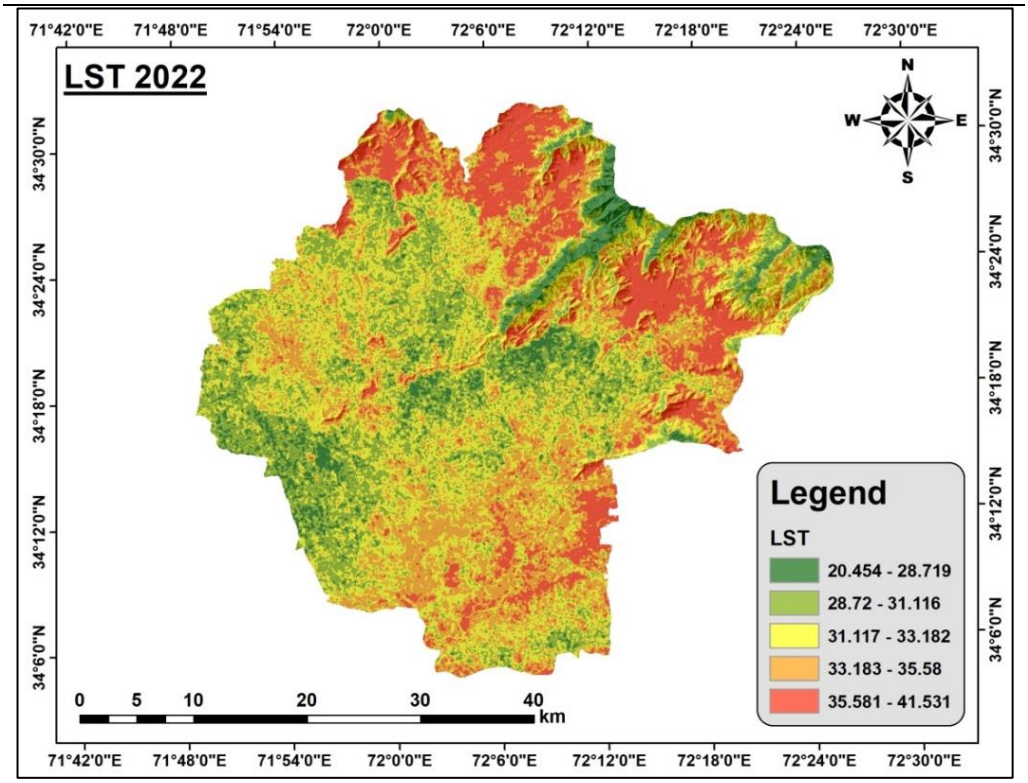

Figure 7: LST Map of 2022

Spatio-Temporal Changes in LST from 2002 to 2022:

The examination of Land Surface Temperature (LST) changes in District Mardan, Khyber Pakhtunkhwa, from 2002 to 2022 reveals significant transitions across various temperature classes. Understanding these changes is crucial for effective environmental management and policymaking.

Transition from Barren Land (BA) to Built-up Land (BU):

Approximately 50.70 km², or about 3.10% of the total area, of previously undeveloped land has been converted into built-up areas between 2002 and 2022. This shift highlights urban growth and infrastructure development over the past 20 years, driven primarily by economic expansion and population growth. The map illustrates these changes with orange patches representing areas where urbanization has replaced unused or sparsely vegetated land.

Transition from Barren Land (BA) to Vegetation Land (VG):

Approximately 177.63 km², or 10.85% of the total area, has transitioned from barren to vegetated land. This change could be attributed to reforestation efforts, agricultural expansion, or natural vegetation restoration. Increasing plant cover is vital for improving ecological balance,

enhancing biodiversity, and reducing soil erosion. This shift reflects a growing awareness of the importance of green spaces.

Transition from Barren Land (BA) to Water Bodies (WB):

There has been a noticeable but less dramatic change, with around 12.38 km² (0.76% of the total area) of barren land converted into water bodies. This change may result from new water management projects such as ponds or reservoirs designed to meet irrigation needs and enhance water availability. While less significant compared to other changes, these modifications are important for local water resource management.

Transition from Vegetation Land (VG) to Barren Land (BA):

Approximately 95.59 km², or 5.84% of the total area, has shifted from vegetated to barren land. This degradation could be due to natural disasters, overgrazing, unsustainable farming practices, or deforestation. Addressing these issues through land rehabilitation and sustainable management practices is essential to counteract the loss of vegetation.

Transition from Vegetation Land (VG) to Built-up Land (BU):

Red patches on the map indicate areas that have been converted from vegetation to built-up land, covering approximately 146.16 km², or 8.93% of the total area. This reflects urban sprawl into formerly agricultural or wooded regions. While indicative of economic development, it underscores the need for well-planned urban expansion that balances growth with environmental preservation.

Transition from Water Bodies (WB) to Barren Land (BA):

Approximately 1.97 km², or 0.12% of the total area, has seen a conversion from water bodies to barren land. This shift may be due to water depletion, sedimentation, or the drying up of water bodies, potentially exacerbated by climate change. Protecting existing water resources is crucial for maintaining hydrological balance and supporting local ecosystems.

Transition from Water Bodies (WB) to Vegetation Land (VG):

Around 0.96 km², or 0.06% of the total area, has seen a conversion from water bodies to terrestrial vegetation. This may be due to the reduction in water bodies or infill processes, leading to vegetation growth. While beneficial for native species, this shift highlights the importance of monitoring changes in water resource availability.

Land Surface Temperature (LST) Changes from 2002 to 2022:

The data shows a general increase in LST in District Mardan. The shift from lower to higher temperature classes is particularly evident, with large areas transitioning from "Very Low" (VL) and "Low" (L) to "Medium" (M), "High" (H), and "Very High" (VH) temperature classes. Approximately 519.70 km² of the region has moved to warmer temperature classes, while about 218.49 km² has cooled. This overall temperature rise, driven by urbanization and land use changes, is highlighted by the detailed LST class transitions in Table 3.

Very Low LST Class to Other LST Classes:

The "Very Low" (VL) temperature class saw minimal change, with 37.10 km² (2.27%) remaining in this category. However, shifts from VL to warmer classes indicate a trend toward increasing temperatures. For instance, 40.94 km² (2.50%) transitioned to "Low" (L), and 37.39 km² (2.28%) to "Medium" (M). Notably, 25.44 km² (1.55%) shifted to "High" (H), and 6.04 km² (0.37%) to "Very High" (VH), reflecting areas with rapid warming, likely due to human activities such as urbanization and deforestation.

Low LST Class to Other LST Classes:

The "Low" (L) temperature class experienced diverse transitions. About 28.32 km² (1.73%) shifted from "Low" to "Very Low" (VL), suggesting some cooling, possibly due to reforestation or reduced human activity. A substantial area of 129.69 km² (7.92%) remained in the "Low" class, indicating stable temperatures. Shifts to "Medium" (M) covered 172.25 km² (10.52%), while 107.25 km² (6.55%) moved to "High" (H) and 30.44 km² (1.86%) to "Very High" (VH), indicating increased warming, possibly from new infrastructure development.

Moderate LST Class to Other LST Classes:

The "Moderate" (M) temperature class displayed various transitions. About 21.06 km² (1.29%) cooled to "Very Low" (VL), possibly due to effective land management. Additionally, 133.53 km² (8.16%) transitioned to "Low" (L), suggesting some cooling. However, 180.15 km² (11.01%) remained in the "M" class, showing minimal fluctuation. Substantial warming occurred, with 131.41 km² (8.03%) moving to "High" (H) and 48.22 km² (2.95%) to "Very High" (VH), likely due to industrialization and urbanization.

High LST Class to Other LST Classes:

The "High" (H) temperature class experienced notable transitions. Approximately 9.75 km² (0.60%) cooled from "High" to "Very Low" (VL), indicating successful temperature reduction in some areas. Additionally, 50.90 km² (3.11%) shifted to "Low" (L), showing slight cooling. Transitions to "Medium" (M) covered 92.68 km² (5.66%), reflecting minor temperature decreases. However, 118.63 km² (7.25%) remained in the "H" class, while 88.94 km² (5.43%) transitioned to "Very High" (VH), indicating significant warming, likely due to increased urbanization.

Very High LST Class to Other LST Classes:

Changes in the "Very High" (VH) temperature class highlight significant impacts. Around 3.03 km² (0.19%) cooled from "VH" to "Very Low" (VL), potentially due to effective environmental restoration. A transition from "VH" to "Low" (L) covered 6.13 km² (0.37%), while 11.89 km² (0.73%) shifted to "Medium" (M). Significant cooling was noted with 43.85 km² (2.68%) moving to "High" (H), but a large area of 81.82 km² (5.00%) remained in the "VH" class, showing minimal temperature change.

Table 4: LST Changes in Classes from 2002 - 2022

Class 2002	Class 2022	Change Classes	Change Area SqKm	Change %
VL	VL	VL To VL	37.10	2.27
VL	L	VL To L	40.94	2.50
VL	M	VL To M	37.39	2.28
VL	H	VL To H	25.44	1.55
VL	VH	VL To VH	6.04	0.37
L	VL	L To VL	28.32	1.73
L	L	L To L	129.69	7.92
L	M	L To M	172.25	10.52
L	H	L To H	107.25	6.55
L	VH	L To VH	30.44	1.86
M	VL	M To VL	21.06	1.29
M	L	M To L	133.53	8.16
M	M	M To M	180.15	11.01
M	H	M To H	131.41	8.03
M	VH	M To VH	48.22	2.95
H	VL	H To VL	9.75	0.60
H	L	H To L	50.90	3.11
H	M	H To M	92.68	5.66
H	H	H To H	118.63	7.25
H	VH	H To VH	88.94	5.43
VH	VL	VH To VL	3.03	0.19
VH	L	VH To L	6.13	0.37
VH	M	VH To M	11.89	0.73
VH	H	VH To H	43.85	2.68
VH	VH	VH To VH	81.82	5.00

Measurement of Coefficient of Determination for LST with Normalized Satellite Indices:

Table 7 illustrates the annual fluctuations in Land Surface Temperature (LST) for the Mardan region in 2002 and 2022, as derived from various normalized satellite indices. The data reveals a significant increase in LST variability over the past two decades. This annual fluctuation is notably more pronounced when compared to indices such as the Normalized Difference Built-up Index (NDBI), Soil Adjusted Vegetation Index (SAVI), Normalized Difference Vegetation Index (NDVI), and Bare Soil Index (BI).

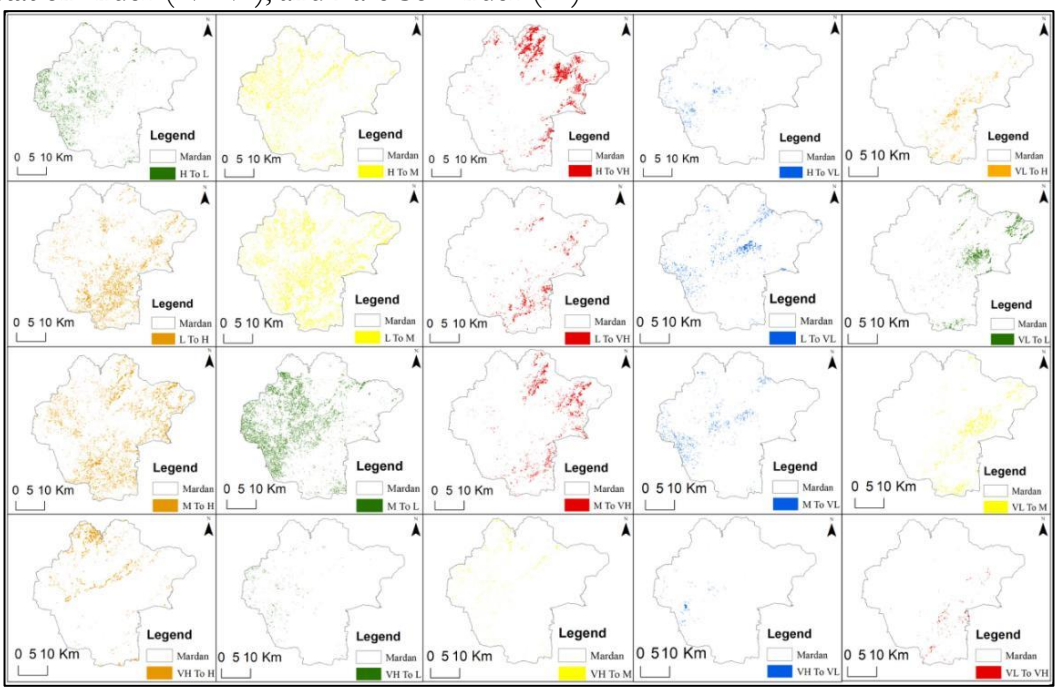

Figure 8: LST Changes in Classes from 2002 – 2022

LST and indicators like SAVI, NDBI, and BI exhibited a statistically significant positive association from 2002 to 2022, particularly in Mardan City. This suggests that as urbanization and soil exposure increased, so did LST, indicating higher temperatures in areas with less vegetation and more built-up infrastructure. Conversely, a negative correlation was observed between LST and NDVI and NDWI, indicating that cooler temperatures were more common in regions with greater vegetation and water resources. This trend highlights how the presence of greenery and water bodies can mitigate urban heat.

There have been unfavorable trends in LST in Mardan's western and higher regions. The significant temperature increases in areas with diminished vegetation underscore the crucial role of green cover in moderating urban heat. Conversely, a small area in Mardan's eastern and lower regions showed an inverse correlation with NDVI, suggesting that the limited vegetation made it challenging to accurately assess LST patterns in these areas.

Overall, the robust annual relationship between LST and the various indices underscores the complex interplay between surface temperatures, vegetation cover, and urban expansion. By 2022, the association between LST and these indicators demonstrated a 75.4% increase in positive trends, highlighting the significant impact of environmental factors and urbanization on Mardan's temperature variations.

LST and NDVI:

2002: A substantial negative correlation (R^2 = -0.6530) was observed between LST and NDVI, indicating that higher NDVI values, which reflect denser vegetation, were associated with lower LST levels. This suggests that vegetation plays a role in cooling the surface.

2022: The negative correlation persisted but weakened to −0.5453, suggesting that the cooling effect of vegetation has diminished, likely due to increased urbanization reducing available green space.

LST and NDWI:

2002: A somewhat positive correlation (R^2 = 0.4140) was noted between LST and NDWI. This might seem unusual since water bodies generally have a cooling effect; however, this positive association could be attributed to urban heat islands near water bodies, leading to higher temperatures in these areas.

2022: The correlation weakened to 0.2142, reflecting a weak positive link. This variability might result from changes in land use near water bodies or specific meteorological conditions during the study period.

LST and SAVI:

2002: A strong negative correlation (R^2 = -0.7250) was found between LST and SAVI, suggesting that lower LST was associated with higher SAVI values, indicative of healthier vegetation with minimal soil impact.

2022: The correlation weakened significantly to 0.1354, indicating that the role of soil-adjusted vegetation in cooling the surface has diminished, possibly due to increased urbanization and reduced green space.

LST and NDBI:

2002: A very strong positive correlation (R^2 = 0.8910) was observed between LST and NDBI, reflecting the significant impact of urban areas on land surface temperatures.

2022: The correlation increased to 0.9927, suggesting that built-up areas are contributing even more to higher temperatures, indicating an intensification of the urban heat island effect.

Table 5: LST with Normalized Indices soil may be a factor in rising temperatures.

Year	Indi	LST	NDVI	NDWI	SAVI	NDBI	BI
2002	LST	1.0000	-0.6530	0.4140	-0.7250	0.5931	0.7580
	NDV	-0.7320	1.0000	-0.7841	0.9085	-0.8671	-0.8282
	NDI	0.6321	-0.7746	1.0000	0.8510	-0.8157	-0.7819
	SAVI	-0.7203	0.9078	-0.8487	1.0000	-0.8813	-0.9265
	NDB	0.8871	-0.8656	0.6555	-0.9288	1.0000	0.9477
	BI	0.7510	-0.8281	0.5979	-0.9228	0.9918	1.0000
2022	LST	1.0000	−0.5453	0.2142	0.1354	0.6672	0.6564
	NDV	−0.5453	1.0000	−0.7087	1.0000	−0.7791	−0.8248
	NDI	−0.1609	−0.7087	1.0000	−0.7214	0.1481	0.8252
	SAVI	0.7354	1.0000	−0.7214	1.0000	−0.7698	0.4390
	NDB	0.9927	−0.7791	0.1481	−0.7798	1.0000	0.6073
	BI	0.7564	−0.8248	0.8252	0.3247	0.2633	1.0000

LST and BI:

2002: A strong positive correlation (R^2 = 0.7580) between LST and BI indicates that higher LST values are associated with areas of greater bare soil, reflecting the influence of bare soil on increasing surface temperatures.

2022: The correlation weakened to 0.6564, showing a moderately favorable link between LST and BI. While bare soil still impacts LST, the effect appears diminished, likely due to increased urbanization and changes in land use.

Calculation of LST from Urban Indices:

The linear regression model used to predict Land Surface Temperature (LST) based on urban indices (UI) is illustrated in Figure 9. The model reveals a substantial connection between LST and UI, with an R^2 value of 0.89, indicating a significant relationship. This robust correlation

suggests that despite potential saturation issues affecting indices like NDVI, the relationship between LST and UI remains strong. As UI values increase, LST also tends to rise.

The linear regression model was validated using Landsat data from 2022, confirming its alignment with established temperature trends, as shown in Figure 8. The model compared temperatures derived from the model (Tmod) with those observed by satellites (Tsat). This analysis, which involved data from 300 locations within the study area, incorporated Landsat 8 thermal data and UI temperature readings, as detailed in Figure 9. The successful comparison demonstrated the model's capability to accurately forecast temperature fluctuations.

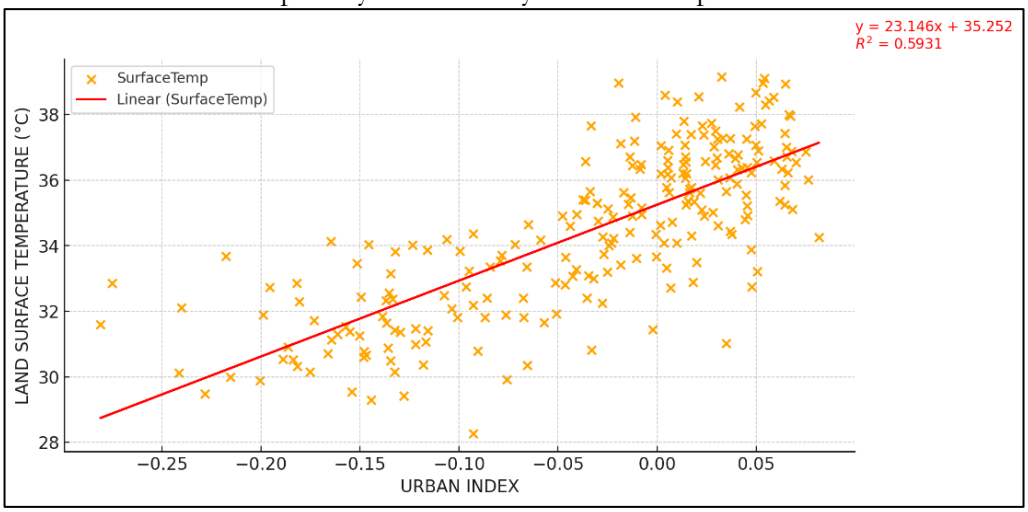

Figure 9: Linear Regression Model LST and UI

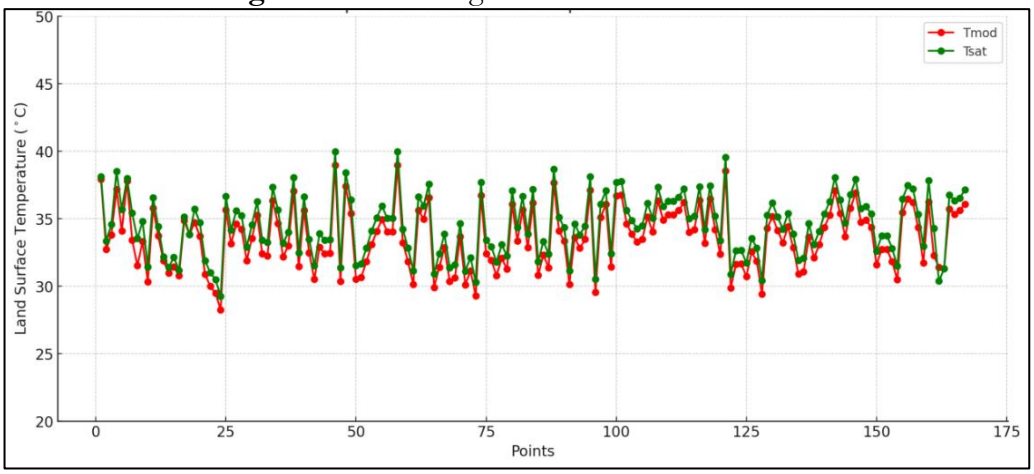

Figure 10: Comparisons between TMOD and TSAT

LST and LULC Prediction for 2042:

Prediction and Distribution of LULC and LST in Mardan 2042:

LULC 2042:

Figure 11 presents the projections from the CA-Markov chain model, illustrating the expected changes in land use and land cover (LULC) by 2042. The model predicts a significant expansion of populated areas, encroaching upon natural landscapes, vegetation, and water bodies. If current trends persist, green spaces are likely to be increasingly replaced by urban infrastructure, as has been observed in the past. **Table 8** highlights a substantial increase in the area occupied by built-up regions by 2042. Specifically, the model forecasts a reduction in vegetation from 793.09 km² in 2022 to 747.66 km² by 2042, while built-up areas are expected to expand from 266.70 km² to 299.99 km². This growth in urban regions, coupled with the decline in water bodies, vegetation, and bare land, emerges as the key drivers of future land cover changes.

Table 6: Area Statistics of Predicted LULC for 2042

Classes Names	Area in Km²	Percentage %
Water Bodies	38.3228	2.34
Vegetation	747.6607	45.65
Built-up	299.9938	18.32
Barren Land	551.8851	33.70

Changes from 2022 to 2042 in Land Use Land cover:

The CA-Markov model projects significant changes in Mardan's land cover between 2022 and 2042. Notably, the northwest corner of the region is expected to undergo a substantial transition from barren land to developed, built-up areas, accounting for approximately 24.2 square kilometers, or 1.48% of the total area. Additionally, 20.9 square kilometers, or 12.28%, of previously undeveloped land is projected to become vegetated. The conversion of bare land to water bodies (BA to WB) is minimal, affecting just 0.76 square kilometers, or 0.05% of the area.

In the northern section, a significant shift is anticipated from vegetated land to barren land (VG to BA), impacting about 25.7 square kilometers, or 1.57% of the total area. Similar transitions from vegetated to built-up regions are expected in the central and eastern sections, covering 20.9 square kilometers, or 1.28% of the area. Changes from water bodies to barren land (WB to BA) are negligible, influencing only half a square kilometer, or 0.03%. This spatially-driven study highlights the dynamic and evolving nature of Mardan's land cover due to ongoing urbanization and shifts in land use patterns.

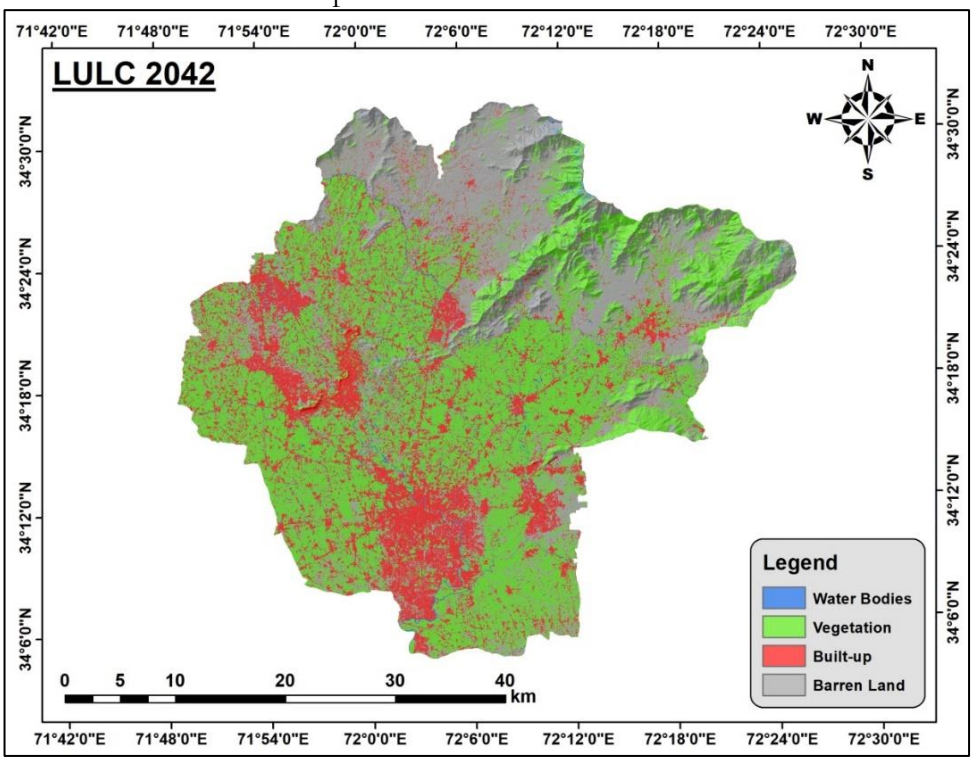

Figure 11: Predicted LULC from CA Markov Model for 2042

LST 2042:

The projected trend in land surface temperature (LST) from 2022 to 2042 is illustrated in Figure 11. The model attributes the fluctuations in LST during this period to the expansion of built-up areas. As high LST zones (exceeding 35.581°C) are expected to increase, the lower LST categories are anticipated to diminish. Vegetated areas in the western region are likely to remain cooler compared to urbanized areas. Higher LST classes (31.117–33.182°C, 33.183–

35.58°C, and 35.581–41.531°C) are predicted to gradually replace regions currently characterized by lower LST ranges (20.454–28.719°C and 28.72–31.116°C). According to Table 4, significant temperature increases are most likely in the southern, northern, and northeastern regions, with many areas potentially transitioning into higher temperature categories (above 35.581°C).

Table 7: Changes of different LULC classes which are predicted from CA Markov

Classes 2022	Classes 2042	Change Classes	Change Area SqKm	Change %
Barren Land	Barren Land	No Change	475.75	29.06
Barren Land	Built-up	BA To BU	24.20	1.48
Barren Land	Vegetation	BA To VG	20.88	1.28
Barren Land	Water Bodies	BA To WB	0.76	0.05
Built-up	Built-up	No Change	263.55	16.10
Vegetation	Barren Land	VG To BA	47.79	2.92
Vegetation	Built-up	VG To BU	47.97	2.93
Vegetation	Vegetation	No Change	711.23	43.45
Water Bodies	Barren Land	WB To BA	9.58	0.59
Water Bodies	Vegetation	WB To VG	4.57	0.28
Water Bodies	Water Bodies	No Change	30.57	1.87

The model forecasts a reduction in the 20.454–28.719°C temperature range from 100.05 km² to 84.8367 km² between 2022 and 2042, while the 35.581–41.531°C LST range is expected to expand from 256.14 km² to 320.8833 km². Over time, temperatures in the higher range (above 35.581°C) are anticipated to increase, encroaching upon the lower temperature categories. This trend is clearly illustrated in Figure 11, showing a significant rise in temperatures within populated areas. Most low LST zones (20.454–28.719°C and 28.72–31.116°C) are projected to shift into higher LST categories (33.183–35.58°C and 35.581–41.531°C). Consequently, while the area of lower LST may shrink, many regions, particularly in the center, north, northwest, and northeast, are likely to experience a shift toward higher temperatures, exceeding 35.581°C as indicated in Table 8.

Table 8: Area statistics of predicted LST for 2042

Classes Range	Area in Km²	Percentage %
20.454 - 28.719 (VL)	84.8367	5.18
28.72 - 31.116 (L)	327.3489	20.00
31.117 - 33.182 (M)	461.2779	28.18
33.183 - 35.58 (H)	442.5156	27.03
35.581 - 41 .531 (VH)	320.8833	19.60

Changes in LST from 2022 to 2042:

Significant regional variations in Mardan's land surface temperature (LST) are projected from 2022 to 2042. Areas initially classified as very low (VL) temperatures are expected to transition, with 4.57 km² shifting to moderate (VL to M) and 4.26 km² to high temperatures (VL to H), accounting for 0.28% and 0.26% of the total area, respectively. Additionally, a very small region of 0.03 km², representing about 0.002% of the area, is projected to shift from very low to very high temperatures (VL to VH). Low-temperature (L) zones are also expected to undergo significant changes, with 13.6 km² (0.83% of the total area) moving to high temperatures (L to H) and 6.8 km² (0.42%) shifting to moderate temperatures (L to M). Notably, 13.3 km² in central Mardan and 0.2 km² in northern Mardan are anticipated to see transitions from moderate to high and very high temperatures, respectively (M to H and VH).

Furthermore, 2.4 km², or 0.15% of the landmass, is expected to experience a shift to very high temperatures (VH), indicating a substantial change from high temperatures (H). Over the next two decades, several parts of Mardan are expected to see a rise in land surface temperatures, reflecting the impact of urbanization and potential climate change factors. This

trend towards higher temperature classes highlights the influence of these factors on local temperature variations.

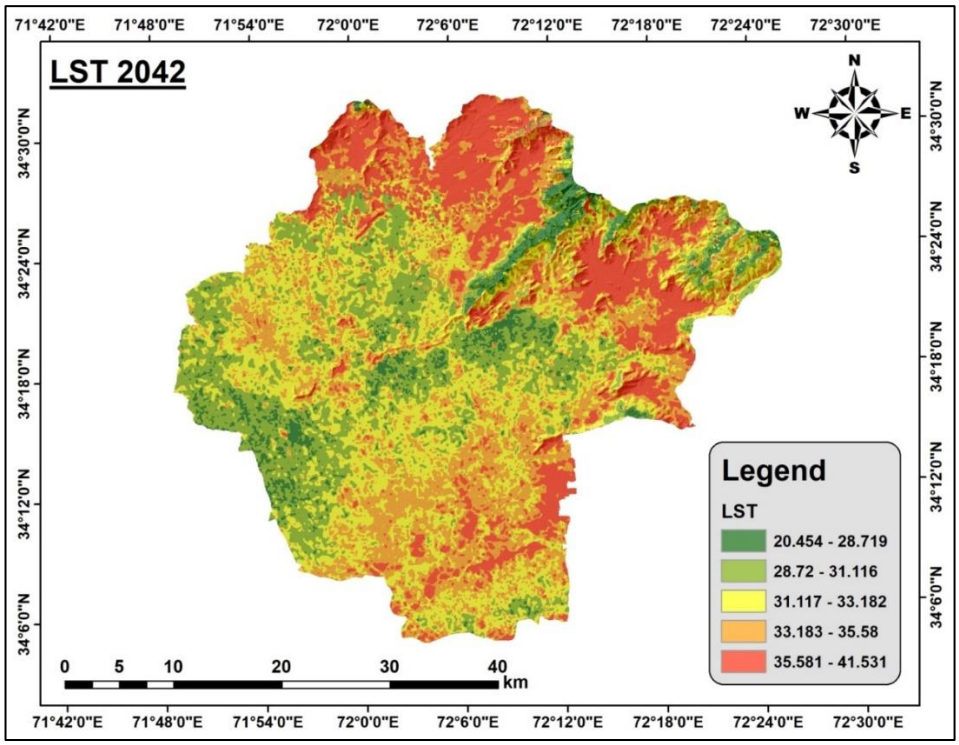

Figure 12: Predicted LST from CA Markov Model for 2042

Table 9: Changes of different LST classes which are predicted from CA Markov

Class 2022	Class 2042	Change Classes	Change Area (Sq.Km)	Change %
VL	VL	VL To VL	81.65	4.99
VL	L	VL To L	8.67	0.53
VL	M	VL To M	4.57	0.28
VL	H	VL To H	4.26	0.26
VL	VH	VL To VH	0.03	0.00
L	VL	L To VL	2.68	0.16
L	L	L To L	280.34	17.13
L	M	L To M	54.29	3.32
L	H	L To H	16.67	1.02
L	VH	L To VH	7.16	0.44
M	VL	M To VL	0.11	0.01
M	L	M To L	38.48	2.35
M	M	M To M	392.35	23.97
M	H	M To H	39.60	2.42
M	VH	M To VH	23.56	1.44
H	VL	H To VL	0.00	0.00
H	L	H To L	0.01	0.00
H	M	H To M	11.12	0.68
H	H	H To H	376.63	23.01
H	VH	H To VH	38.86	2.37
VH	H	VH To H	4.61	0.28
VH	VH	VH To VH	250.87	15.33

Discussions: This study utilized Markov chain models based on cellular automata to predict land use, land cover (LULC), and land surface temperature (LST) in Mardan, Khyber

Pakhtunkhwa, Pakistan. The analysis assessed the predictive power of various land cover indices in forecasting temperature changes over time. Among the indices—Soil-Adjusted Vegetation Index (SAVI), Normalized Difference Vegetation Index (NDVI), Normalized Difference Built-up Index (NDBI), and Built-up Index (BI)—the Normalized Difference Water Index (NDWI) emerged as the most accurate predictor of LST distribution.

Linear regression techniques were employed to predict the expansion of urban centers and the corresponding temperature changes. Multiple linear regressions were deemed suitable as long as there was no collinearity among the predictor variables. The Urban Index (UI) proved to be the most accurate predictor of temperature, considering the interdependence of other factors. The UI model was used to predict urbanization growth and its future trajectory, calculating the potential environmental impact on LST. The model predicted temperatures with an average absolute error of 1.83 °C, using LST data from the thermal band combined with the UI in a linear model. Recent studies have confirmed a strong correlation between the UI's accuracy in forecasting heat patterns from urban growth and various measures of urban expansion.

While previous research had not fully established the link between temperature and UI, the higher temperatures observed in areas with more built-up infrastructure and less vegetation can be attributed to the significant predictive power demonstrated in this study. Similar patterns have been observed in Colombo and Sri Lanka, where urban indices are high in residential and water-intensive areas. The strong correlation between UI and LST can be explained by studies showing that urban climates significantly impact residential water and energy consumption. In 1990 and 2018, the Support Vector Machine (SVM) classifier was employed to achieve high-accuracy classification of urban land use and land cover (LULC) distribution. Recent studies also demonstrated the SVM classifier's capability to produce highly accurate maps. By using digitized areas rather than points as the ground data for classification, a map was created with precision exceeding the required 80% accuracy level.

LULC maps from 2002 and 2022 revealed that while residential areas expanded, vegetation cover in the same area decreased, a finding consistent with earlier research. The high degree of agreement between the 2022 projected map and the map produced using supervised classification techniques validates the accuracy of the CA-Markov chain model in predicting land cover and land use categories. The CA-Markov chain model forecasts continued growth of built-up areas until 2042 at the expense of natural land cover, unless policies are implemented to promote green spaces, cropland, and water conservation. This prediction aligns with global trends indicating that human population growth will continue to outpace the expansion of natural areas. The study also predicted an increase in areas with higher temperatures (31–35 °C and 35–41 °C), while regions with the lowest temperature levels are likely to decrease. As urbanization intensifies, green space and water availability will diminish, mirroring patterns observed in previous studies.

The study's findings are crucial for reshaping urban planning and management in Khyber Pakhtunkhwa. Addressing issues such as land record management, solid waste management infrastructure, capacity building, landfill construction, pond removal, and support for local governments in rehabilitating hazardous buildings will enhance the district's urban resilience.

Conclusion:

The spatiotemporal analysis of Land Use and Land Cover (LULC) in Mardan from 2002 to 2022 reveals significant changes driven by urbanization. The study found a substantial increase in built-up areas from 165.47 km² to 266.70 km², at the expense of vegetative and agricultural lands, which decreased from 928.76 km² to 793.09 km² during the same period. These changes highlight the ongoing trade-off between urban expansion and the preservation of natural land cover. The overall accuracy (OA) of the study improved from 81% in 2002 to 87% in 2022, demonstrating the reliability of the Maximum Likelihood Classification (MLC)

algorithm used in the analysis. The environmental impact of increased urbanization is underscored by the reduction in vegetative cover and the rise in arid and built-up areas.

Moreover, LST data indicates a discernible trend of rising temperatures over the past two decades, with the average LST range shifting from 25–36°C in 2002 to 20–41°C in 2022, and higher temperatures becoming more prevalent. The positive correlation between LST and urban indices (UI) suggests a direct relationship between the expansion of built-up areas and the reduction of vegetative cover, contributing to the observed temperature increases. CA-Markov model projections for 2042 indicate a continued rise in built-up areas, reaching 299.99 km², while vegetative cover is expected to decline to 747.66 km². The model also predicts an increase in high LST zones, with certain areas potentially experiencing temperatures above 35.58°C. These projections emphasize the urgent need for sustainable urban design and environmental conservation measures to mitigate the adverse effects of urbanization on climate and land use. The study underscores the importance of integrating green spaces and water bodies into urban development plans to balance growth with environmental sustainability. The findings provide valuable insights into the dynamic changes in land use and temperature in the Mardan region and can guide policymakers in making informed decisions to enhance urban sustainability and resilience amid ongoing development and climate challenges.

References

[1] S. Liu et al., "Understanding Land use/Land cover dynamics and impacts of human activities in the Mekong Delta over the last 40 years," Glob. Ecol. Conserv., vol. 22, p. e00991, Jun. 2020, doi: 10.1016/J.GECCO.2020.E00991.

[2] M. M. H. Seyam, M. R. Haque, and M. M. Rahman, "Identifying the land use land cover (LULC) changes using remote sensing and GIS approach: A case study at Bhaluka in Mymensingh, Bangladesh," Case Stud. Chem. Environ. Eng., vol. 7, p. 100293, Jun. 2023, doi: 10.1016/J.CSCEE.2022.100293.

[3] E. F. Lambin and H. Geist, Eds., "Land-Use and Land-Cover Change," 2006, doi: 10.1007/3-540-32202-7.

[4] "(PDF) Land use/land cover change detection and prediction using the CA-Markov model: A case study of Quetta city, Pakistan." Accessed: Jun. 22, 2024. [Online]. Available: https://www.researchgate.net/publication/355209516_Land_useland_cover_change_detection_and_prediction_using_the_CA-Markov_model_A_case_study_of_Quetta_city_Pakistan

[5] "Urban Climate | Journal | ScienceDirect.com by Elsevier." Accessed: Jun. 22, 2024. [Online]. Available: https://www.sciencedirect.com/journal/urban-climate

[6] "Temporal March of the Chicago Heat Island in: Journal of Applied Meteorology and Climatology Volume 24 Issue 6 (1985)." Accessed: Jun. 22, 2024. [Online]. Available: https://journals.ametsoc.org/view/journals/apme/24/6/1520-0450_1985_024_0547_tmotch_2_0_co_2.xml

[7] X. L. Chen, H. M. Zhao, P. X. Li, and Z. Y. Yin, "Remote sensing image-based analysis of the relationship between urban heat island and land use/cover changes," Remote Sens. Environ., vol. 104, no. 2, pp. 133–146, Sep. 2006, doi: 10.1016/J.RSE.2005.11.016.

[8] R. Wang, H. Hou, Y. Murayama, and A. Derdouri, "Spatiotemporal Analysis of Land Use/Cover Patterns and Their Relationship with Land Surface Temperature in Nanjing, China," Remote Sens. 2020, Vol. 12, Page 440, vol. 12, no. 3, p. 440, Jan. 2020, doi: 10.3390/RS12030440.

[9] P. Ghosh et al., "Application of Cellular automata and Markov-chain model in geospatial environmental modeling- A review," Remote Sens. Appl. Soc. Environ., vol. 5, pp. 64–77, 2017, doi: 10.1016/j.rsase.2017.01.005.

[10] B. Nath, Z. Wang, Y. Ge, K. Islam, R. P. Singh, and Z. Niu, "Land Use and Land Cover

Change Modeling and Future Potential Landscape Risk Assessment Using Markov-CA Model and Analytical Hierarchy Process," ISPRS Int. J. Geo-Information 2020, Vol. 9, Page 134, vol. 9, no. 2, p. 134, Feb. 2020, doi: 10.3390/IJGI9020134.

[11] D. J. Guan, H. F. Li, T. Inohae, W. Su, T. Nagaie, and K. Hokao, "Modeling urban land use change by the integration of cellular automaton and Markov model," Ecol. Modell., vol. 222, no. 20–22, pp. 3761–3772, Oct. 2011, doi: 10.1016/J.ECOLMODEL.2011.09.009.

[12] X. Yang, X. Q. Zheng, and L. N. Lv, "A spatiotemporal model of land use change based on ant colony optimization, Markov chain and cellular automata," Ecol. Modell., vol. 233, pp. 11–19, May 2012, doi: 10.1016/J.ECOLMODEL.2012.03.011.

[13] J. Huang, Y. Wu, T. Gao, Y. Zhan, and W. Cui, "An Integrated Approach based on Markov Chain and Cellular Automata to Simulation of Urban Land Use Changes," Appl. Math. Inf. Sci, vol. 9, no. 2, pp. 769–775, 2015, doi: 10.12785/amis/090225.

[14] F. Fan, Y. Wang, and Z. Wang, "Temporal and spatial change detecting (1998-2003) and predicting of land use and land cover in Core corridor of Pearl River Delta (China) by using TM and ETM+ images," Environ. Monit. Assess., vol. 137, no. 1–3, pp. 127–147, Jun. 2008, doi: 10.1007/S10661-007-9734-Y/METRICS.